COVER SHEET

Paper Number: **409**

Title: **3D Representative Volume Element Reconstruction of Fiber Composites via Orientation Tensor and Substructure Features**

Authors: Yi Li[1, 2]
Wei Chen[1]
Hongyi Xu[3*]
Xuejun Jin[2, 4]

[1] Department of Mechanical Engineering, Northwestern University, Evanston, IL 60208, USA
[2] Institute of Advanced Steels and Materials, School of Materials Science and Engineering, Shanghai Jiao Tong University, Shanghai 200240, China
[3] Research and Advanced Engineering, Ford Motor Company, Dearborn, MI 48126, USA
[4] Collaborative Innovation Center for Advanced Ship and Deep-Sea Exploration, Shanghai Jiao Tong University, Shanghai 200240, China
* Corresponding author: Dr. Hongyi Xu, hxu41@ford.com

(FIRST PAGE OF ARTICLE – *align this to the top of page – leave space blank above ABSTRACT*)

ABSTRACT

To provide a seamless integration of manufacturing processing simulation and fiber microstructure modeling, two new stochastic 3D microstructure reconstruction methods are proposed for two types of random fiber composites: random short fiber composites, and Sheet Molding Compounds (SMC) chopped fiber composites. A Random Sequential Adsorption (RSA) algorithm is first developed to embed statistical orientation information into 3D RVE reconstruction of random short fiber composites. For the SMC composites, an optimized Voronoi diagram based approach is developed for capturing the substructure features of SMC chopped fiber composites. The proposed methods are distinguished from other reconstruction works by providing a way of integrating statistical information (fiber orientation tensor) obtained from material processing simulation, as well as capturing the multiscale substructures of the SMC composites.

1. INTRODUCTION

Fuel efficiency and low carbon emission regulations are playing a major role in raising the demand for lightweight composite automotive components to replace the traditional metal parts. Fiber composites materials are identified as one of the most promising candidates for automotive lightweighting due to the competitive mechanical properties, non-toxic, fast cycle times and part consolidation potential [1-3]. There are two types of fiber composites: long fiber (unidirectional or woven) composites, and short fiber composites. The short fiber composites have the advantages of the processing ease and a relatively low processing cost compared to the continuous fiber composites. Furthermore, both isotropic and anisotropic properties can be achieved in short fiber composites. In this work, we focus on modeling the microstructure of short random-fiber composites. Based on the 'Processing-Microstructure-Property' modeling chain [4], numerous efforts in materials experiment [5, 6] and simulation [7-12] are carried out to achieve high performance short random-fiber composites materials by carefully controlling material microstructures through appropriate manufacturing process. The property of short random fiber composites materials highly depends on microstructure features such as aspect ratio, volume fraction, orientation, and substructure. However, modeling and simulating of short random-fiber composites materials properties via materials microstructures are still fields of active research, yet to be fully explored.

To expand the use of random-fiber composites materials, accurate prediction of materials constitutive behavior is required. Three major categories of methods have been introduced [7]. The first category is the analytical homogenization method based on Eshelby's strain concentration tensor [13]. Fibers are modeled as the second phase inclusions in the resin matrix. This method is applicable to the prediction of fiber composites properties with unidirectional fiber distribution. and it can also be extended

to account for random orientations by embedding orientation averaging process [14]. The second category of methods are based on the classical laminated plate theory (CLPT) where fiber material is approximated as a set of parallel layers of in-plane randomly oriented fibers. This method is computationally powerful in modeling fiber composites with laminated structure [1]. However, the aforementioned two categories of methodologies are limited in assessing nonlinear material properties, because those methods are lacking a quantitative description of the complex microstructure or a statistical description of the uncertainties in microstructure and material properties. The third category is the microstructure-based Finite Element Analysis (FEA) method. Advanced finite element technologies enable the direct material property evaluation on a Representative Volume Element (RVE).

RVE explicitly captures the materials' geometrical features on the micro-level. RVE-based FEA analysis has been widely accepted in 2D material property simulation, however, some material properties such as the anisotropy of material, the stress transfer effect and the inter-filler interaction can only be accurately captured in 3D [8]. There exists even less works on 3D RVE reconstruction of short random-fiber materials' microstructure, due to the high complexity in the micro-architectures, such as random orientation distribution, irregularly shaped substructures, high compactness induced by a large fiber volume fraction, large fiber aspect ratios, and fiber curvature. To this end, the challenge is how to generate digital microstructure reconstructions of short fiber composites in 3D space. The statistically equivalent reconstructions match the pre-specified microstructure statistical information, which are obtained from either image-based microstructure characterization or material processing simulations.

There are three major categories of RVE reconstruction methods for the random fiber system. The first category is based on the Random Sequential Adsorption (RSA) algorithm. This algorithm is firstly introduced in [15]. Objects (e.g. fibers) are generated and placed in the cubical space iteratively. There is no overlapping between the objects. The principle of RSA is quite straightforward and easy to apply in the random-fiber system. The fibers and fiber tows are usually represent by ellipsoids, cylinders or straight lines. Bohm et al. [16] introduced a modified RSA approach and generated RVEs of metal matrix composites. The fiber entities are represented by arrangements of identical cylindrical, spheroidal or spherical reinforcements. The fiber orientation distribution is purely random in the RVE model. Tu et al. [17] applied a similar RSA approach and generated RVEs to simulate the thermo-conductivity and elastic modulus behavior of fiber composites. The fiber volume fraction is up to about 30% while overlapping is allowed in the RVE. The fiber orientation distribution is again purely random in the RVE model. Kari et al. [18] proposed a modified RSA which sequentially places different sizes of fibers in the RVE to achieve a high fiber volume fraction. However, the generated fiber size distributions are not realistic. Pan et al. [19] employed a modified RSA algorithm and generated a RVE of a random-fiber composite with fibers entity represented by long cylinder. The fibers are placed in sublayers, which are subsequently stacked to generate a 3D body. The fiber volume fraction is 13.5%. In a more recent work of Pan et al. [7], fiber kinks are introduced to achieve a higher fiber volume fraction and to avoid overlapping. The resulting volume fraction is 35%−40%. However, the fiber kinks structure is not realistic. Furthermore, the fiber orientation is generated randomly in the 2D XY-plane without a component in the Z direction.

The second category of reconstruction methods are Monte Carlo-based methods. Firstly an initial configuration of arbitrary fibers' locations and orientations is created.

Secondly, the fibers are rearranged following certain rules to eliminate overlapping. Gusev et al. [20, 21] used the Monte Carlo-based method in modeling material properties of short fiber reinforced composites. The fiber volume fraction and aspect ratio limits are similar to the RSA method and again there is no specific orientation information embedded in the Gusev`s model, i.e., the fiber orientation distribution is purely random.

The third category is the image analysis-based method. With the microscopy techniques such as scanning electron microscopy (SEM) and confocal microscopy [22] or X-ray tomography [23], the fiber microstructure features can be observed and quantified from the microstructures. Gerd et al. [9, 24] generated a multi-layer model of fiber composites on the basis of 2D SEM information and validate the model by comparing to the 3D information obtained by the synchrotron tomography. The reconstructed model matches quite well with the synchrotron tomography information with respect to the microstructure statistics. In the work of Faessel et al. [25], microstructure images are obtained by synchrotron radiation tomography. The 3D fiber RVE is reconstructed based on the X-ray absorption radiographs. However the statistical information of microstructure features, especially the fiber orientation distribution, is not representative because of small window sizes of the 2D microscopic images. On the other hand, the synchrotron radiation tomography can only generate exactly the same microstructure as the specific material sample. In computational material design, it is important to generate a large number of statistically equivalent microstructure models for quantifying the uncertainties in the microstructure and the resultant properties. Furthermore, the tomography techniques are expensive and demanding on the sample preparation.

As summarized above, the existing RSA or Monte Carlo-based microstructure reconstruction methods do not consider the statistical fiber orientation information in reconstructions. It is assumed that the fibers are distributed randomly in the 2D or 3D space. However, the fiber orientation has a significant effect on the material properties of fiber composites [5, 26-28]. The patterns of fiber orientation distribution are strongly influenced by the processing methods and conditions. Great efforts have been made in predicting the evolution of fiber orientation distribution during material processing [10, 29]. The elastic properties of fiber composites have been predicted analytically from the fiber orientation information [11, 12]. However, the analytical method is limited in handling plastic properties while predicting large deformation behavior is urgent for fiber composites materials. This calls for a solution to embed statistical fiber orientation information into the RVE for subsequent finite element analysis. Furthermore, existing models fail to capture the special microstructure features of Sheet Molding Compounds (SMC), where the microstructure of SMC is featured by the random distribution of fiber tows, formed by dozens of aligned fibers (Figure 7 (a-c)).

The purpose of this paper is to develop 3D stochastic reconstruction methods to enable the 3D modeling of both random fiber composites and the SMC chopped fiber composites. The remainder of this paper is organized as follows: In Section 2, the general framework of the proposed 3D RVE reconstruction for fiber composites materials is introduced. In Section 3, the basic knowledge of orientation tensor and the principle of recovering the fiber probability distribution function (PDF) from orientation tensor are briefly reviewed as a part of the technical background. In Section 4, an improved RSA model is introduced to illustrate how to employ the statistical fiber orientation information (PDF) in the reconstruction of random fiber composites. In

Section 5, a Voronoi diagram-based two-level reconstruction algorithm is proposed for the reconstruction of SMC chopped fiber composites. A case study is done as a demonstration of the proposed Voronoi diagram-based algorithm. For the time being the processing modeling and FEM simulation work are still in process and are not included in this paper. Section 6 concludes the paper.

2. FRAMEWORK FOR RANDOM SHORT FIBER 3D RVE RECONSTRUCTION

The proposed framework for random fiber 3D RVE reconstruction includes four main steps, as shown in Figure 1. In Step 1, key microstructure descriptors are identified as the quantitative representation of microstructure features based on the available information from processing simulation and microstructure images. In Step 2, key microstructure descriptors are quantified. For example, the fiber orientation probability distribution function is recovered from the fiber orientation tensor (Section 3) and descriptors such as aspect ratio are quantified based on image analysis. In Step 3, statistically equivalent RVE are reconstructed in the 3D space (Sections 4 and 5). In Step 4, the reconstructed RVE is validated by comparing the input statistical information and that of the reconstructed RVEs (Section 4.2 and Section 5.4).

The proposed methods can be distinguished from any other existing works in two regards: (1) The statistical fiber orientation tensor obtained from processing simulation (e.g. compression molding, injection molding) is considered in microstructure reconstruction; and (2) The tow structure features of SMC are captured.

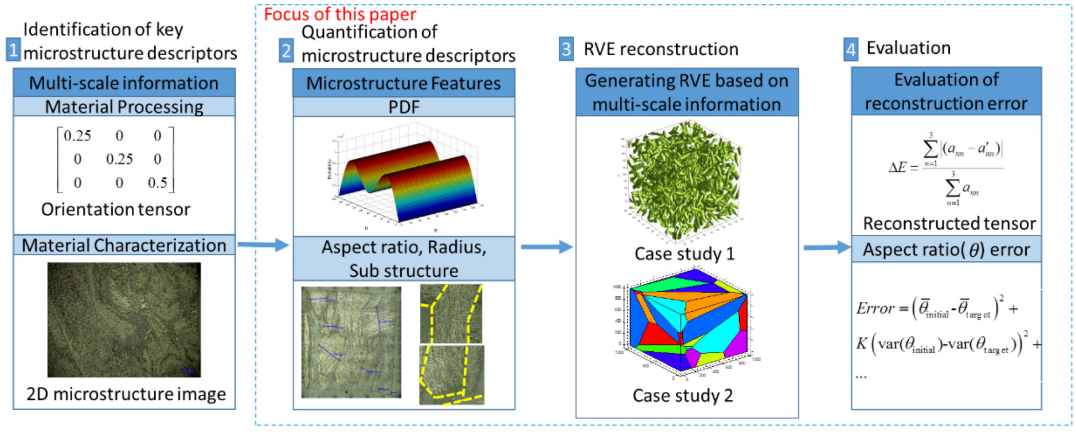

Figure 1. Framework for random short fiber 3D RVE reconstruction

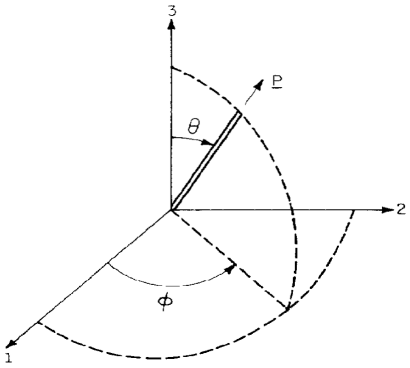

Figure 2. Cartesian coordinate system for random short fiber 3D RVE reconstruction

3. RECOVERY OF FIBER ORIENTATION DISTRIBUTION FROM ORIENTATION TENSOR MATRIX

Orientation of a single short fiber can be represented by the angles **(θ, φ)** as shown in Figure 2. Hence, the orientation state of a point in space can be described by a Probability Distribution Function (PDF) **ψ(θ, φ)**. The probability of finding a fiber with the two angles between θ_1 and $\theta_1+d\theta$, and φ_1 and $\varphi_1+d\varphi$, are given by

$$P(\theta_1 \le \theta \le \theta_1 + d\theta, \phi_1 \le \phi \le \phi_1 + d\phi) = \psi(\theta_1, \phi_1)\sin\theta_1 d\theta d\phi \tag{1}$$

In Cartesian coordinate system, orientation of a single short fiber can be equivalently represented by a unit vector $\mathbf{P}= (P_1, P_2, P_3)$, thus one can write the distribution function **ψ(P)** as a function of **P**. The three components of vector **P** are given by

$$p_1 = \sin\theta\cos\phi \tag{2a}$$

$$p_2 = \sin\theta\sin\phi \tag{2b}$$

$$p_3 = \cos\theta \quad . \tag{2c}$$

3.1 The concept of fiber orientation tensor

The PDF is too verbose for numerical calculations of three-dimensional fiber orientation in complex geometries [10, 29]. Orientation tensor, especially the second-order tensor, a much compact description of fiber orientation as defined in the following has been widely used in the calculation of fiber orientation in flow molding process.

The most commonly used second-order and fourth-order orientation tensors are:

$$a_{ij} = \oint_S p_i p_j \psi(\boldsymbol{P}) d\boldsymbol{P} \quad , \tag{3a}$$

$$a_{ijkl} = \oint_S p_i p_j p_k p_l \psi(\boldsymbol{P}) d\boldsymbol{P} \tag{3b}$$

where S is the surface of the unit sphere. From the definition, it is evident that orientation tensors are symmetric and has the following normalized properties:

$$a_{ij} = a_{ji} \tag{4a}$$

$$a_{ii} = 1 \quad . \tag{4b}$$

The lower order tensor can be derived from higher order tensor as:

$$a_{ijkk} = a_{ij} \tag{5a}$$

$$a_{ijklmm} = a_{ijkl} \quad . \tag{5b}$$

3.2 Recovery of fiber orientation distribution function

As mentioned above, orientation tensor is low order orientation information of orientation distribution. To construct a microstructure RVE, the fiber orientation probability distribution function needs to be recovered from the fiber orientation tensor matrix following the formulation developed by Tucker et al. [14]. By expanding the distribution function in orthogonal functions of the components of $\boldsymbol{P}$:

$$\psi(\boldsymbol{P}) = \frac{1}{4\pi} + \frac{15}{8\pi} b_{ij} f_{ij}(\boldsymbol{P}) + \frac{315}{32\pi} b_{ijkl} f_{ijkl}(\boldsymbol{P}) + \ldots \quad , \tag{6}$$

where b_{ij} , b_{ijkl} are the deviatoric versions of the orientation tensors:

$$\delta_{ij} = \begin{cases} 0 & , \quad \mathrm{i} \neq \mathrm{j} \\ 1 & , \quad \mathrm{i} = \mathrm{j} \end{cases} \tag{7a}$$

$$b_{ij} = a_{ij} - \frac{1}{3}\delta_{ij} \tag{7b}$$

$$\begin{aligned} b_{ijkl} = a_{ijkl} &- \frac{1}{7}(\delta_{ij}a_{kl} + \delta_{ik}a_{jl} + \delta_{il}a_{jk} + \delta_{jk}a_{il} + \delta_{jl}a_{ik} + \delta_{kl}a_{ij}) \\ &+ \frac{1}{35}(\delta_{ij}\delta_{kl} + \delta_{ik}\delta_{jl} + \delta_{il}\delta_{jk}) \end{aligned} \quad , \tag{7c}$$

and $f_{ij}(\boldsymbol{P})$, $f_{ijkl}(\boldsymbol{P})$ are tensor basis functions of $\boldsymbol{P}$.

$$f_{ij}(\boldsymbol{P}) = p_i p_j - \frac{1}{3}\delta_{ij} \ , \tag{8a}$$

$$\begin{aligned} f_{ijkl}(\boldsymbol{P}) = p_i p_j p_k p_l &- \frac{1}{7}(\delta_{ij}p_k p_l + \delta_{ik}p_j p_l + \delta_{il}p_j p_k + \delta_{jk}p_i p_l + \delta_{jl}p_i p_k + \delta_{kl}p_i p_j) \\ &+ \frac{1}{35}(\delta_{ij}\delta_{kl} + \delta_{ik}\delta_{jl} + \delta_{il}\delta_{jk}) \end{aligned} \quad . \tag{8b}$$

As shown in equation (6), one needs infinite set of orientation tensors to fully recover the distribution function. However, this form provides an approximation of the distribution function with a finite set of orientation tensors by truncating the series in equation (6). The higher the order of information is included in the recovery, a higher accuracy will be obtained. Since most processing simulations only keep the second-order tensor as the orientation state variable, in this paper the distribution function is recovered from only the second-order tensor and the forth-order tensor. The second-order tensor is the orientation state directly obtained from the processing simulation and the forth-order tensor is the closure approximation based on the second-order tensor. There are two ways to form the closure approximation [14]. The first one is the linear

closure approximations which are exact for a completely random distribution of fiber orientation：

$$a_{ijkl} = \frac{1}{7}(\delta_{ij}a_{kl} + \delta_{ik}a_{jl} + \delta_{il}a_{jk} + \delta_{jk}a_{il} + \delta_{jl}a_{ik} + \delta_{kl}a_{ij}) - \frac{1}{35}(\delta_{ij}\delta_{kl} + \delta_{ik}\delta_{jl} + \delta_{il}\delta_{jk}) . \quad (9)$$

The second one is the quadratic closure approximation which is exact for the perfect uniaxial alignment of fibers.

$$a_{ijkl} = a_{ij}a_{kl} \ . \quad (10)$$

By mixing the quadratic and linear forms according to some microstructure image measurements of orientations, one can get a more accurate approximation:

$$\overline{a}_{ijkl} = (1-f)a^{L}_{ijkl} + f a_{ijkl} \ , \quad (11)$$

where f is a generalization of Herman's orientation factor; it is equal to zero for randomly oriented fibers and unity for perfectly aligned fibers. Orientation tensor and orientation distribution function do not have one-to-one mappings. For a specific orientation tensor, changing the value of f will lead to a different resultant distribution. There are several candidate approximation algorithms for converting tensor to PDF. In this paper f is taken as zero to build RVE with a more randomly distribution nature. One can get a more aligned distribution by increasing the value of f [30]. Figure 3 shows two examples of the PDF recovered through orientation tensor.

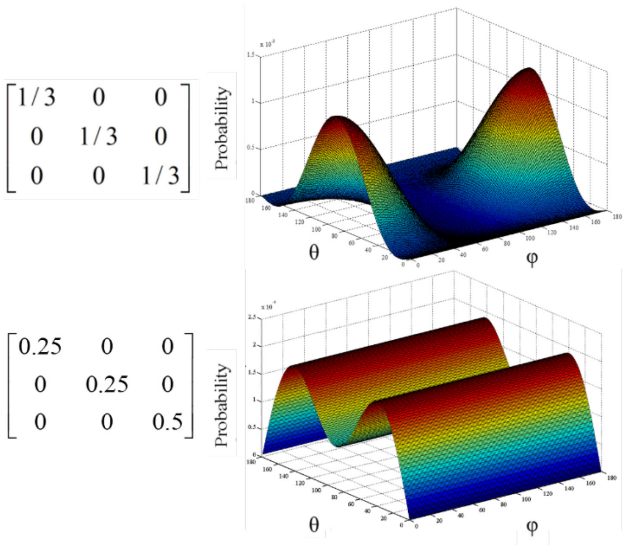

Figure 3. Orientation tensor and the corresponding Probability Distribution Function

4. 3D RVE RECONSTRUCTIONS OF RANDOM SHORT FIBER COMPOSITES

4.1 An improved RSA algorithm for random short fiber composites reconstruction

Traditionally, the Random Sequential Adsorption (RSA) algorithms do not take fiber orientation distribution into consideration, so they can only generate pure randomly distributed-composite microstructures. In this work, an improved RSA algorithm is developed to generate statistically equivalent random microstructures that match the input fiber orientation distribution. The details of the algorithm are demonstrated as following (Figure 4):

1) Input fiber parameters: The fibers are represented by cylinders with the same diameter and length. The input of the reconstruction algorithm includes: fiber diameter, fiber length, number of fibers and the PDF of fiber orientation.
2) Determine fiber orientation: The fiber orientation is generated based on the PDF retrieved from fiber orientation tensor as explained in Section 3. Orientations with higher probability in the PDF are more likely to be chosen.
3) Determine the location of fiber ends: One end of a fiber is randomly generated. Then the nearest distance between the newly generated fiber and the existing fibers are calculated and compared to the fiber predefined diameter. If there is overlap of fibers, the fiber location will be re-picked until there is no overlap. By tuning the threshold of the nearest distance one can control the density of the fiber.
4) Fibers are generated and placed into the 3D space sequentially. The non-overlapping constraint must be satisfied in the generation process, i.e., each point in the RVE space cannot be occupied by more than one fiber.
5) Stopping criterion: The algorithm will stop either when the number of fibers reaches a predefined value, or when fiber generating (Step 3 and 4) has been tried unsuccessfully for a predefined number of times, which usually happens when the volume fraction is high and close to its upper limit when using the RSA method [1, 13, 16, 31].

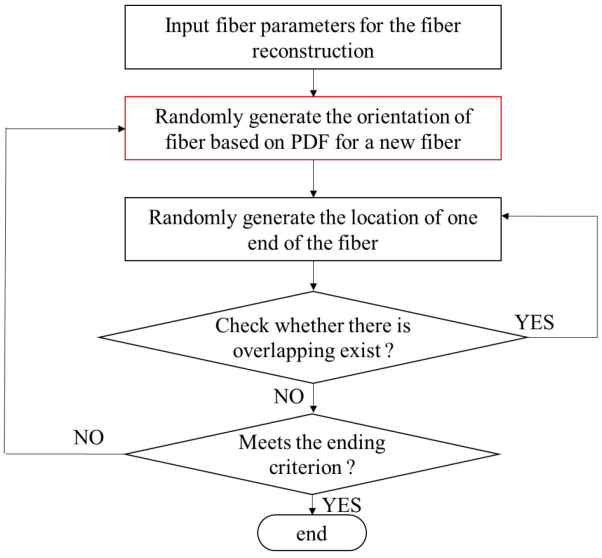

Figure 4. Flow chart of the RVE generation algorithm for random short fiber composites

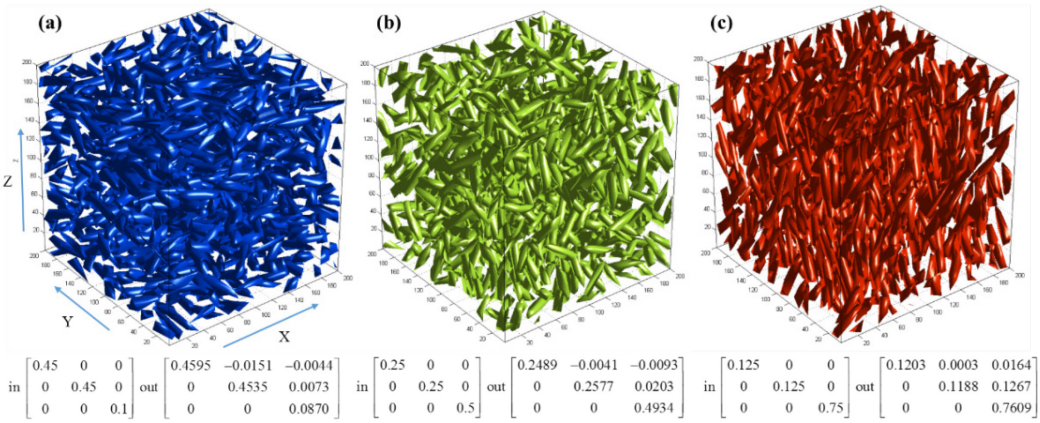

Figure 1. 3D RVE achieving different targets of input fiber orientation tensor

4.2 Case study 1: Reconstruction of random short fiber composites with specific fiber orientation distribution

To illustrate the improved RSA algorithm, three different second order orientation tensors are used for demonstration. They correspond to three typical fiber orientation distribution patterns. In Figure 5, the length and diameter of a fiber are defined as 20 and 5, respectively. 650 fibers are generated in each RVE to ensure a relative compact reconstruction with a small orientation tensor error which will be assessed in Section 4.3. The fiber volume fraction (VF) information is summarized in Table I. Even though higher VF can be achieved by adding more fibers (more than 650), this is not the focus of this work.

According to Equation (3), a higher eigenvalue of the components of the tensor indicates a higher probability distribution of fiber in the relative orientation. For the first case (Figure 5 (a)), the input tensor orientation tensor with eigenvalues (0.45, 0.45, and 0.1) corresponds to an almost transversely isotropic RVE with only little tendency aligned along the Z direction. For the second case (Figure 5 (b)), the input tensor orientation tensor with eigenvalues (0.25, 0.25, and 0.5) corresponds to a more randomly distributed fiber RVE. For the third case (Figure 5 (b)), the input orientation tensor with eigenvalues (0.125, 0.125, and 0.725) corresponds to an almost vertically aligned fiber distribution. The input orientation tensor (in) and the actual orientation tensor (out) of the reconstructed RVEs are listed in Figure 5. As shown in Figure 5, fibers distribute mainly transversely in Figure 5 (a). Fibers distribute randomly in Figure 5 (b). Fibers distribute vertically along Z direction in Figure 5 (c). Our tests confirm that the fiber distribution in the reconstructed RVE matches well with the three input orientation tensors.

4.3 Validation of the RVE reconstructions

The reconstructed 3D random short fiber RVE is validated by comparing the reconstruction's fiber orientation tensor matrix to the target orientation tensor matrix. A perfect reconstruction will have zero error in such comparison:

$$\Delta E = \frac{\sum_{n=1}^{3} \left| (a_{nn} - a'_{nn}) \right|}{\sum_{n=1}^{3} a_{nn}} \quad , \tag{12}$$

where ΔE is the orientation tensor error, a_{nn} is the input second order orientation tensor and a'_{nn} is the orientation tensor of the reconstructed RVE. The orientation tensor error of the three RVEs in Figure 5 is summarized Table 1. As it can be noted, the error is very small and negligible.

The statistical distribution of fiber orientation cannot be matched accurately unless there are a sufficient number of fibers. Increasing the number of fibers in a RVE, the reconstruction error of orientation tensor will decrease. However, a larger number of fibers also lead to a shorter distance between fibers, which require a finer mesh for the resin phase. It will increase the computational cost of FEM. To achieve a balance between the accuracy and the computational cost, the convergence relation between the orientation tensor error and the number of fibers is demonstrated using the case of orientation tensor eigenvalue (0.25, 0.25, 0.5). Reconstructions of different numbers of fibers are generated with this orientation tensor, and then the error of the reconstructed orientation tensor is calculated by Equation (3), as shown in Figure 6. It is evident that the error of orientation distribution converges to zero as the number of fibers increases: $\Delta E = 4.6\%$ for 32 fibers and $\Delta E = 0.9\%$ for 512 fibers. Therefore, it is concluded that less than 1% error in fiber orientation tensor can be achieved with 512 fibers. Further increasing the number of fibers will not decrease the orientation error significantly (Figure 6).

Table 1. Summary of the information for the three reconstructions

RVE	Num of fiber	components in orientation tensor			VF(%)	ΔE(%)
		a_{11}	a_{22}	a_{33}		
a	650	0.45	0.45	0.1	18.1	2.30
b	650	0.25	0.25	0.5	17.1	1.34
c	650	0.125	0.125	0.75	18.3	2.18

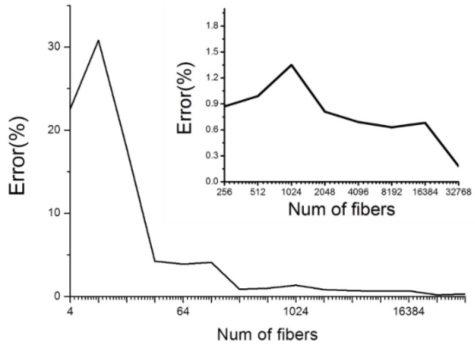

Figure 2. Orientation error vs. Number of fiber

5. 3D RVE RECONSTRUCTION OF SMC CHOPPED FIBER COMPOSITES

5.1 Fiber tow structures features of SMC chopped fiber material

The raw materials of SMC include resin and carbon/glass fiber bundles. The diameter of the fiber is 10~14 μm, and the length of the fiber bundle is around 25mm. In the fabrication process, the fiber bundles are chopped into short fiber tows, which are mixed with resin by a series of processing steps including compounding, thicken and compression moulding [32]. Figure 5.1 (a) shows a typical SMC microstructure. Different from short random fiber composites, two important features of SMC are observed: 1) The microstructure consists of randomly-oriented fiber tows; 2) Each fiber tow consists of aligned fibers. All fibers have the same orientation inside each fiber tow. Instead of tracing the orientation angle of each fiber, the fiber orientation is represented by the statistical distribution of fiber tow orientations weighted by the fiber tow area.

5.2 Concept of Voronoi diagram

In the proposed SMC reconstruction algorithm, the concept of Voronoi diagram is used to partition a whole space into subareas, each represents different orientations of fiber tows. In mathematics, a Voronoi diagram is a partitioning of a space into regions based on distance to points in a specific subset of the space. That set of points (called seeds, sites, or generators) are specified beforehand, and for each seed there is a corresponding region consisting of all points closer to that seed than to any other. These regions are called Voronoi cells. Figure 7 (d) shows an example of 2D Voronoi diagram with 15 Voronoi cells. As highlighted in Figure 7 (b-c), the geometry of SMC's sub-structure (fiber tow), is similar to the Voronoi cells. Therefore, we propose to use Voronoi cells to represent the fiber tows in the RVE reconstruction. The key question here is how to adjust the shape of Voronoi cells to match the statistical distribution of the fiber tows' geometry. In Section 5.3, an optimization-based reconstruction algorithm is developed to generate Voronoi cells based on pre-specified size and aspect ratio. Once the reconstruction is partitioned into multiple cells, the fiber orientation of each cell is then assigned to match the predefined fiber orientation tensor. In FEA simulations of composite properties, the properties of UD composites are assigned to each fiber tow (Figure 7 (e)). The UD properties are predicted from the virtual tensile tests on UD RVE, which has the same fiber VF as the SMC fiber tows.

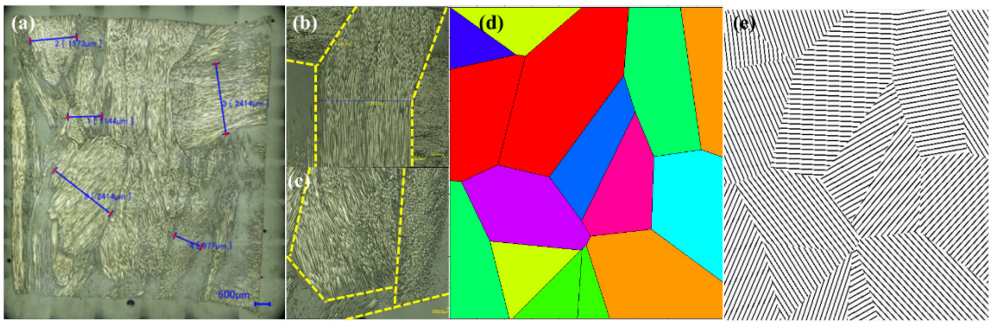

Figure 7 (a) Microstructures of SMC fiber materials, (b-c) fiber tows and boundaries highlighted in yellow, (d) 2D Voronoi diagram with 15 cells, (e) 2D reconstruction to capture the features in (a)

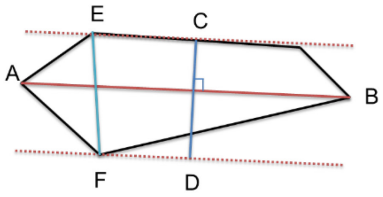

The long axis of a Voronoi cell (fiber bundle) is defined as the longest distance between its vertices i.e. the line AB.
The short axis is defined as the line CD.

$$|CD| = \frac{\overrightarrow{EF} \times \overrightarrow{AB}}{|AB|}$$

$$Cella\ spect\ ratio = \frac{|AB|}{|CD|}$$

Figure 8. Illustration of the shape parameters of Voronoi cells and fiber tows

5.3 Tow structure reconstruction using Simulated Annealing (SA) optimization

The shape of a fiber tow is quantified by two parameters: tows area/volume and the aspect ratio of the tows. The definition of aspect ratio in 2D is illustrated in Figure 8. Such definition can be easily extended for 3D cases.

An optimization-based algorithm is introduced for reconstructing the tow structure (Figure 9). First, the number of cells is defined and an initial Voronoi diagram is generated by randomly arranging the seeds into the 2D or 3D reconstruction space. The shapes of Voronoi cells are determined by the seed locations. A Simulated Annealing (SA) algorithm is employed to move the seeds to the optimal locations such that the sizes and aspect ratios of the Voronoi cells match the predefined distributions with the least error. During each iteration in the SA optimization, the location of one randomly selected seed is randomly perturbed. Subsequently, a candidate Voronoi diagram is generated based on new seed locations. An evaluation of the shape parameters of the fiber tows is conducted to determine whether the statistics of the new structure (the new set of Voronoi cells) is closer to the target. The acceptance criterion is defined in Equation (13).

$$\begin{aligned} E_{candidate} = &\left(\bar{\theta}_{candidate} - \bar{\theta}_{\text{target}}\right)^2 + K_1\left(\text{var}(\theta_{candidate}) - \text{var}(\theta_{\text{target}})\right)^2 \\ &+ I\left[\left(\bar{V}_{candidate} - \bar{V}_{\text{target}}\right)^2 + K_2\left(\text{var}(V_{candidate}) - \text{var}(V_{\text{target}})\right)^2\right], \end{aligned} \tag{13a}$$

$$\Delta E = E_{candidate} - E_{current} \tag{13b}$$

$$P = \exp(-\Delta E / kt) \tag{13c}$$

where $\bar{\theta}_{candidate}$ and $\bar{V}_{candidate}$ are the mean aspect ratio and volume of the new set of Voronoi cells, respectively. $\bar{\theta}_{\text{target}}, \bar{V}_{\text{target}}$ are the mean aspect ratio and volume of the target Voronoi cells. In addition, the variance of the volume and aspect ratio are also matched. var(...) stands for the variance calculator. I, K_1, K_2 are the weighting factors, and kt is the annealing factor. In this paper, we recommend to use $K_1 = K_2 = 30, kt = 0.01$. ΔE is the energy error. $\Delta E < 0$ indicates that the candidate Voronoi diagram is closer to the target.

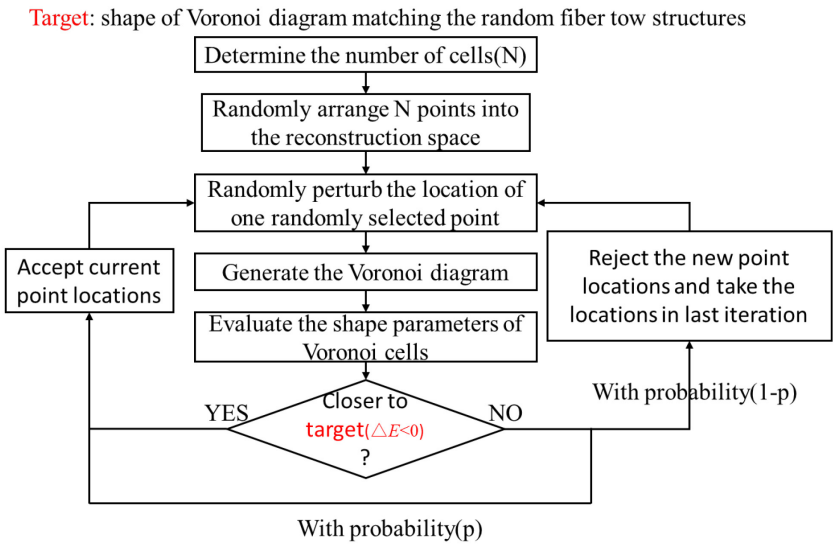

Figure 9. Flowchart of the optimization-based reconstruction algorithm

If $\Delta E < 0$, the perturbed structure will be accepted as the new candidate structure; if $\Delta E > 0$ the perturbed structure will be accepted with a small probability P. P will decrease as the number of iteration increases (Equation (13)). Acceptance of a worse structure with a small probability enables the optimal search not be trapped in local optimums. The algorithm will stop either when $E_{current}$ decreases to a predefined value, or when the run time limit is reached.

As fibers have the same orientation inside each fiber tow, the calculation of orientation tensor is modified as:

$$a_{ij} = \int_S p_i p_j \psi(\boldsymbol{P}) A_k d\boldsymbol{P} \quad , \tag{14}$$

where A_k is the area of the kth cell. After the reconstruction is partitioned into multiple cells, the fiber orientation of each cell is then assigned to match the predefined fiber orientation tensor.

5.4 Case study 2: reconstruction of SMC chopped fiber composites

In this section, the optimization-based SMC microstructure reconstruction algorithm is demonstrated on a 3D case. By conducting image-based characterization on the microscopic images of the SMC composites, the values of two input microstructure descriptors can be determined: the mean area of the Voronoi cells, and the mean and variance of the Voronoi cell's aspect ratio. Given the total area of the microstructure, the number of Voronoi cells can be calculated as the total area divided by the mean cell area. In this work, the number of Voronoi cells is 32. The target mean of aspect ratio is set as 2.5, the target variance of aspect ratio is set as 0.01 and the target variance of cell volume is set as 10e+12. The shape parameters in this study are unitless such that it can be mapped to any unit system easily. The total volume of the RVE and the number of Voronoi cells are fixed so that the mean of cell volume is determined accordingly. The terms $\left(\overline{V}_{candidate}\text{-}\overline{V}_{\text{target}}\right)^2$ in equation (13) equal to zero.

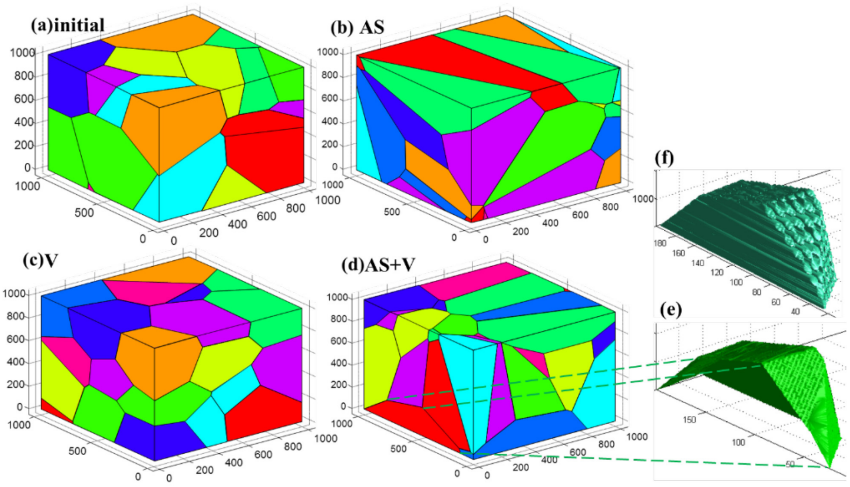

Figure 3. 3D RVE reconstruction of SMC chopped fiber composites. Fiber tows are represented by Voronoi diagram. (a) initial random configuration (b) AS (c) V (d) AS+V (e) surface of one cell in the RVE reconstruction (f) one Voronoi cell filled with aligned fibers

Microstructures created based on different reconstruction targets are compared in Figure 10. Figure 10 (a) is a purely randomly generated RVE. Figure 10 (b) is an RVE reconstruction that only matches the target mean and variance of aspect ratio (AS). Figure 10 (c) is an RVE reconstruction that only matches the mean and variance of cell volume (V). Figure 10 (d) is an RVE reconstruction that matches the target mean and variance of both aspect ratio and cell volume (AS+V). In Table 2 the accuracy of the four RVE reconstructions are compared quantitatively. By comparing the parameters of AS, V, AS+V to those of the initial RVE, it is evident that when taking only a single target parameter into consideration the simulated annealing algorithm works well in reducing the difference between target parameters and the initial parameters. However, there is a tradeoff between meeting the target of cell volume and that of the cell aspect ratio when considering both in the objective function.

Table 2. Parameters of Voronoi cells for the RVEs in Figure 10 (a) initial random configuration (b) RVE reconstruction of matched AS (c) RVE reconstruction of matched V (d) RVE reconstruction of matched AS+V

RVE	$\bar{\theta}(target = 2.5)$	var(θ)($target = 0.1$)	var(V)($target = 10e13$)	I
(a)Random	1.27	0.04	4.14E+14	/
(b)AS	2.53	0.12	3.20E+14	0
(c)V	1.24	0.03	9.02E+13	I>>Ic
(d)AS+V	2.19	0.13	1.42E+14	I=Ic

The fiber orientation of each cell is generated based on the PDF as explained in Sections 3 and 4. For a coarse Finite Element Analysis (FEA), each Voronoi cell is assigned with the property of Unique Directional (UD) fiber composites of the same Volume Fraction. For a more accurate analysis, each Voronoi cell can be filled with aligned fibers entities, as shown in Figure 10 (e-f). It should be noted that a wide range of volume fraction can be achieved by the proposed reconstruction algorithm. Inside each fiber tow, all fibers are oriented to the same direction. The fully aligned fibers don't have the overlapping issue that exists in the random short fiber composites, so there is no fiber volume fraction jamming limit as the RSA method [1, 13, 16, 31]. The highest

volume fraction achieved by RSA is around 30%. The proposed SMC reconstruction has the same VF upper limit as the UD composites: $\frac{\pi}{2\sqrt{3}} \approx 90.6\%$.

6. CONCLUSIONS

In this work, new stochastic 3D microstructure reconstruction methods are developed for both the short random fiber composite and the SMC chopped fiber composites, respectively. These methodologies are fully automated and provide a seamless integration of the manufacturing processing simulation and the fiber microstructure modeling. In the process of 3D RVE reconstruction, statistical fiber orientation information is first recovered from fiber orientation tensor, which is generated as an output from manufacturing process simulation. A random sequential adsorption (RSA) algorithm is developed to embed statistical orientation information into 3D RVE reconstruction of random short fibers. To the authors' best knowledge, this is the first work on stochastic reconstruction of chopped fiber composites considering the statistical orientation information. In addition, an optimized Voronoi diagram based approach is developed for capturing the multiscale substructure features of SMC chopped fiber composites. The Voronoi diagram-based reconstruction is able to achieve high volume fraction of fiber over 50% comparable to values achieved in industrial-grade materials. The limitations of the proposed methods are summarized as the future work. First, the dependency between the fiber orientation and the shape of each cell is not considered in our reconstruction. In the real SMC microstructures, the fibers tend to align parallel to the long axis of the cell. Second, more microscopic information will be obtained to capture the layered structure of SMC in the 3D space.

ACKNOWLEDGEMENTS

This research is supported by US Department of Energy (Award Number: DE-EE0006867) and Ford Motor Company.

REFERENCES

1. Ionita, A. and Y. Weitsman, *On the mechanical response of randomly reinforced chopped-fibers composites: Data and model.* Composites science and technology, 2006. **66**(14): p. 2566-2579.
2. *Composite developments drive auto industry forward.* Reinforced Plastics, 2014. **58**(3): p. 22-25.
3. *Carbon composites and cars – technology watch 2012.* Reinforced Plastics, 2013. **57**(1): p. 39-42.
4. Olson, G.B., *Computational design of hierarchically structured materials.* Science, 1997. **277**(5330): p. 1237-1242.
5. Fu, S.-Y. and B. Lauke, *Effects of fiber length and fiber orientation distributions on the tensile strength of short-fiber-reinforced polymers.* Composites Science and Technology, 1996. **56**(10): p. 1179-1190.
6. Jacob, G.C., et al., *Effect of fiber volume fraction, fiber length and fiber tow size on the energy absorption of chopped carbon fiber–polymer composites.* Polymer Composites, 2005. **26**(3): p. 293-305.
7. Pan, Y., L. Iorga, and A.A. Pelegri, *Numerical generation of a random chopped fiber composite RVE and its elastic properties.* Composites Science and Technology, 2008. **68**(13): p. 2792-2798.
8. Weidt, D. and Ł. Figiel, *Finite strain compressive behaviour of CNT/epoxy nanocomposites: 2D versus 3D RVE-based modelling.* Computational Materials Science, 2014. **82**: p. 298-309.
9. Gaiselmann, G., et al., *3D microstructure modeling of compressed fiber-based materials.* Journal of Power Sources, 2014. **257**: p. 52-64.

10. Han, K.-H. and Y.-T. Im, *Numerical simulation of three-dimensional fiber orientation in short-fiber-reinforced injection-molded parts.* Journal of materials processing technology, 2002. **124**(3): p. 366-371.
11. Chung, S. and T. Kwon, *Numerical simulation of fiber orientation in injection molding of short-fiber-reinforced thermoplastics.* Polymer Engineering & Science, 1995. **35**(7): p. 604-618.
12. Gupta, M. and K. Wang, *Fiber orientation and mechanical properties of short-fiber-reinforced injection-molded composites: Simulated and experimental results.* Polymer Composites, 1993. **14**(5): p. 367-382.
13. Eshelby, J.D. *The determination of the elastic field of an ellipsoidal inclusion, and related problems*. in *Proceedings of the Royal Society of London A: Mathematical, Physical and Engineering Sciences*. 1957. The Royal Society.
14. Advani, S.G. and C.L. Tucker III, *The use of tensors to describe and predict fiber orientation in short fiber composites.* Journal of Rheology (1978-present), 1987. **31**(8): p. 751-784.
15. Widom, B., *Random sequential addition of hard spheres to a volume.* The Journal of Chemical Physics, 1966. **44**(10): p. 3888-3894.
16. Böhm, H.J., A. Eckschlager, and W. Han, *Multi-inclusion unit cell models for metal matrix composites with randomly oriented discontinuous reinforcements.* Computational Materials Science, 2002. **25**(1): p. 42-53.
17. Tu, S.-T., et al., *Numerical simulation of saturation behavior of physical properties in composites with randomly distributed second-phase.* Journal of composite materials, 2005. **39**(7): p. 617-631.
18. Kari, S., H. Berger, and U. Gabbert, *Numerical evaluation of effective material properties of randomly distributed short cylindrical fibre composites.* Computational materials science, 2007. **39**(1): p. 198-204.
19. Pan, Y., L. Iorga, and A.A. Pelegri, *Analysis of 3D random chopped fiber reinforced composites using FEM and random sequential adsorption.* Computational Materials Science, 2008. **43**(3): p. 450-461.
20. Gusev, A.A., *Representative volume element size for elastic composites: a numerical study.* Journal of the Mechanics and Physics of Solids, 1997. **45**(9): p. 1449-1459.
21. Gusev, A., et al., *Orientation averaging for stiffness and thermal expansion of short fiber composites.* Advanced Engineering Materials, 2002. **4**(12): p. 931-933.
22. Page, D. and F. El-Hosseiny, *mechanical properties of single wood pulp fibres. VI. Fibril angle and the shape of the stress-strain curve.* Pulp & paper Canada, 1983.
23. Faessel, M., C. Delisée, and J. Lux. *Microstructure and 3D simulation of wood based fibrous insulators*. in *Second International Conference of the European Society for Wood Mechanics*. 2003.
24. Gaiselmann, G., et al., *Stochastic 3D modeling of fiber-based materials.* Computational Materials Science, 2012. **59**: p. 75-86.
25. Faessel, M., et al., *3D Modelling of random cellulosic fibrous networks based on X-ray tomography and image analysis.* Composites science and technology, 2005. **65**(13): p. 1931-1940.
26. Hine, P., et al., *Measuring the fibre orientation and modelling the elastic properties of injection-moulded long-glass-fibre-reinforced nylon.* Composites Science and Technology, 1995. **53**(2): p. 125-131.
27. Schulgasser, K., *Fibre orientation in machine-made paper.* Journal of materials science, 1985. **20**(3): p. 859-866.
28. Chin, W.K., H.T. Liu, and Y.D. Lee, *Effects of fiber length and orientation distribution on the elastic modulus of short fiber reinforced thermoplastics.* Polymer Composites, 1988. **9**(1): p. 27-35.
29. Folgar, F. and C.L. Tucker, *Orientation behavior of fibers in concentrated suspensions.* Journal of Reinforced Plastics and Composites, 1984. **3**(2): p. 98-119.
30. Advani, S.G. and C.L. Tucker III, *Closure approximations for three-dimensional structure tensors.* Journal of Rheology (1978-present), 1990. **34**(3): p. 367-386.
31. Altendorf, H. and D. Jeulin, *Random-walk-based stochastic modeling of three-dimensional fiber systems.* Physical Review E, 2011. **83**(4): p. 041804.
32. Merhi, D., et al., *Predicting sizing dependent bending rigidity of glass fibre bundles in sheet moulding compounds.* Composites Part A: Applied Science and Manufacturing, 2006. **37**(10): p. 1773-1786.